FINLINES

Finlines are guiding structures for electromagnetic waves that consist of one or several metallic fins suspended in the *E*-plane of a waveguide enclosure. They are the basic transmission media for the so-called integrated *E*-plane circuit technology. The fins can either be suspended freely (metallic *E*-plane lines) or supported by dielectric substrates of low permittivity. The general term "finline" usually applies to the latter type, and there exist many variations that are classified according to the manner in which the metallization is placed on the substrate, and how the planar structure is mounted in the enclosure.

Finlines are applied predominantly in the frequency range between 10 and 100 GHz; but some applications at frequencies up to 170 GHz have been realized. Having losses of typically 0.1 dB per wavelength, finlines are not suitable for long-distance transmission. However, they excel as a circuit medium for millimeter-wave components and systems due to their low manufacturing cost, wide single-mode bandwidth, compatibility with discrete active and passive devices, and suitability for integration with other hybrid circuit techniques as well as with standard rectangular waveguides. Manufacturing costs are moderate for two reasons. First, the planar insert can be fabricated using printed circuit batch processing. Second, since the circuit characteristics are dominated by the topology of the printed insert, dimensional tolerances for the waveguide enclosure can be greatly relaxed (typically by a factor five compared with standard waveguide). The enclosure also prevents radiation losses, reduces susceptibility to outside interference, and may act as a heat sink for active devices. Unfortunately, there is a price to pay for the technological advantages of finlines; their analysis and design are difficult due to the metallic edges that lead to field singularities, the presence of two or more different dielectrics in the structure giving rise to hybrid modes of propagation, and to structural complications necessary for mounting the substrate and for biasing of devices.

A Brief History

Since the early 1940s it has been known that one or two metallic ridges in the *E*-plane of a rectangular waveguide increased its single-mode bandwidth and lowered its characteristic impedance. In particular, Cohn (1) pointed out the potential of this feature for realizing impedance transformers, tapers, filters, slow-wave structures and broadband matched loads by simply changing the ridge depth; Hopfer (2) published extensive and accurate data for the cutoff frequencies, characteristic impedances and power handling capability of ridged waveguides. While the ridge waveguide is not truly quasi-planar, its early theoretical treatment and the manner in which circuit functions were realized have laid the groundwork for the design and realization of finline circuits. In 1955, Robertson (3) built the first truly planar finline component. It was a circular-to-rectangular waveguide coupler fitted with a pair of thin metal fins. Robertson recognized that this technique was suitable for very broadband hybrids, directional and polarization-sensitive couplers. Sixteen years later, Konishi and Hoshino (4) reported a 100 GHz converter featuring a planar metallic circuit in a waveguide. However, the major development in the evolution of *E*-plane technology was Meier's invention of the "integrated finline" in 1972 (5–7), for which he received the Microwave Application Award of the IEEE-MTT society in 1984. By supporting the planar conducting fins with a thin, low-permittivity substrate, Meier extended thin-film fabrication techniques to *E*-plane circuitry and gained additional advantages such as dc isolation of the fins for bias purposes, intermediate frequency (IF) and modulation connections, and mechanical support for discrete devices mounted in parallel or in series with the fins.

Meier's invention spurred intense international research activities and product development. First commercial finline products were announced in the late 1970's. They included mixers, broadband switches, attenuators, detectors and complete integrated radar front ends for frequencies up to 140 GHz (8–12).

CLASSIFICATION OF FINLINES

Finlines can be viewed as derivatives of the four generic structures shown in Fig. 1. In fact, they share some of their characteristics and can be reduced to any of them. A finline is thus created either by placing a slotline into the *E*-plane of a rectangular waveguide, by partially loading a ridge waveguide with dielectric, or by partially metallizing the dielectric in a slab-loaded waveguide. Four basic types of finlines may result; their simplified cross sections are shown in Fig. 2(a) to (d). Insulated, unilateral, bilateral and antipodal finlines can

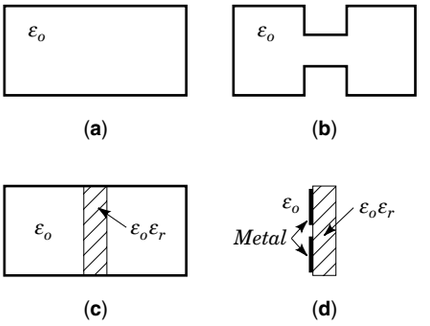

Figure 1. The four generic waveguides from which finlines can be derived. (a) Rectangular waveguide, (b) Double-ridged waveguide, (c) Slab-loaded waveguide, (d) Slotline.

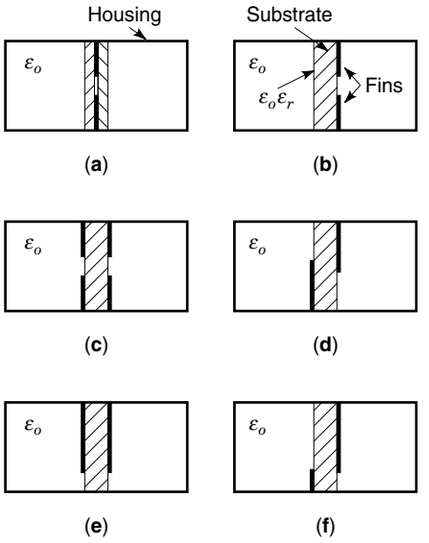

Figure 2. The four basic finline types and some of their variants. (a) Insulated finline, (b) Unilateral finline, (c) Bilateral finline, (d) Antipodal finline (e) Asymmetric bilateral finline, (f) Asymmetric antipodal finline.

be distinguished by the way in which their fins are arranged on the substrate. Further variations of each type are obtained by moving the substrate or the slot away from the symmetrical position, or by adding further planar inserts, strips or slots. For example, Fig. 2(e) and (f) show cross sections of asymmetric finlines.

CONSTRUCTION OF FINLINES

A finline comprises printed metallic fins on a substrate (the planar insert) and a metallic housing that holds the insert and confines the electromagnetic fields. Both soft and hard substrate materials may be used. Glass fiber-reinforced Teflon (RT-duroid™, $\epsilon_r = 2.2$) is the most widely used soft substrate material. It is easily processed and cut, costs little, and has low dielectric permittivity and losses. It is employed mostly at lower millimetric frequencies; a thickness of 0.01 in (0.254 mm) is suitable for components up to 40 GHz, and 0.005 in (0.127 mm) is used for frequencies up to 90 GHz. Finline components and circuits of highest quality and for frequencies beyond 90 GHz call for quartz substrates ($\epsilon_r = 3.75$) which are more expensive, fragile and difficult to process, but provide better mechanical support for delicate semiconductor devices. The housing is usually machined from brass or aluminum in the form of a split-block. Metallized Plexiglas has also been used with mixed results due to adhesion problems. Three housing configurations (Fig. 3) can be found in practice.

The first type has been proposed by Meier (6). Two Π-shaped metal pieces clamp the planar insert [Fig. 3(a)] held in place by nylon screws. Since the substrate extends beyond the confines of the inner waveguide channel, this configuration is partially open. To minimize RF leakage, the clamping region is made $\lambda_d/4$ wide, where λ_d is the wavelength in the dielectric substrate at midband frequency. Furthermore, to suppress the excitation of TEM-type modes in the slot region, longitudinal current flow must be impeded by serrating the substrate metallization in the slot region (42). On the other hand, since one of the fins can be isolated from the housing with a dielectric insert, bias is easily supplied to embedded semiconductor devices.

The second type has been proposed by Adelseck et al. (8). Here, the two halves of the split block touch each other, thus completely shielding the finline [Fig. 3(b)]. A shallow groove is machined into one of the blocks to accommodate the substrate. However, stringent mechanical tolerances (typically ± 10 μm) must be maintained here. If the groove is too wide, poor contact between the fins and the housing can introduce

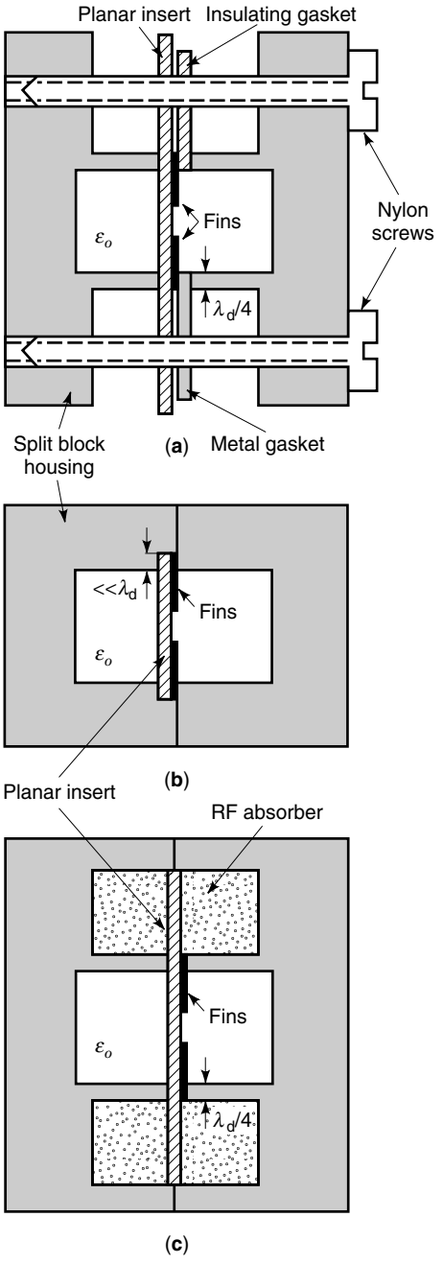

Figure 3. Three types of finline construction. (a) Finline mount proposed by Meier, (b) Finline mount proposed by Adelseck et. al., (c) Combination of (a) and (b) for hard substrates and high frequencies. (After Meier (6), Copyright © 1974 IEEE, reprinted with permission.)

considerable attenuation. If the groove is too narrow, hard substrates may break, and soft substrates may be compressed and pushed out into the waveguide channel, causing bending and possibly rupture of delicate leads of devices. Bias can be fed locally to the clamping region through the metal block, and fins can be insulated from the housing by inserting a thin Mylar sheet into the groove.

The third type combines the features of both approaches [Fig. 3(c)]. It is suitable for quartz substrates at high frequencies (90 GHz and above) where machining tolerances become prohibitive due to the small size of the groove. As in type 1, the walls of the waveguide channel are made $\lambda_d/4$ wide to form a choke, but the substrate protrudes on either side into a secondary channel that contains RF absorbing material. In this way the finline is sealed. Fins can be biased by inserting a thin insulating sheet between fins and housing, and by contacting the fins through a feed connection.

All three techniques have been used successfully in the realization of finline components. Acceleration tests have shown that components of type 2 and 3 with hard substrates can survive up to 30,000 g for 2 ms, while components with soft substrates withstand 2000 g for 0.5 ms or shocks of up to 4000 g (9).

BASIC ELECTROMAGNETIC PROPERTIES OF FINLINES

The most important properties are the propagation constant and the characteristic impedance associated with the dominant mode of propagation. These depend on the geometry of the cross section, the substrate permittivity, and the frequency of operation. Furthermore, the single-mode bandwidth is proportional to the separation between the cutoff frequencies of the dominant and the first higher-order mode. If finline discontinuities are to be analyzed using mode-matching in the longitudinal direction, a significant number of higher-order modes must be characterized as well. While the generic topologies in Fig. 2 yield the characteristics of real finlines quite accurately at lower frequencies, the influence of the geometrical details shown in Fig. 3, such as the substrate mounting grooves and the finite thickness of the metal fins, must be included in the analysis and design of practical components, particularly at higher frequencies where the size of these features is not negligible vis-à-vis the dimensions of the waveguide channel and the substrate thickness.

Similar to regular waveguides, finlines are dispersive, that is their guided wavelength λ_g changes nonlinearly with frequency. In waveguides without partial dielectric filling, the guided wavelength λ_g (or propagation constant β) at any frequency above cutoff can be calculated from the knowledge of the cutoff wavelength λ_c with the well-known formula

$$\lambda_g = \frac{\omega}{\beta} = \frac{\lambda}{\sqrt{1 - (\lambda/\lambda_c)^2}} \tag{1}$$

However, as soon as the waveguide is partially filled with a dielectric material, this formula no longer applies. With increasing frequency, more of the wave energy tends to concentrate inside the material with the higher permittivity, slowing down the propagation velocity. This effect is not included in Eq. (1). To accurately determine the guided wavelength in a finline at any frequency above cutoff, the field problem must be solved separately for each frequency.

As in all waveguides carrying non-TEM waves, voltage and characteristic impedance are not uniquely defined. While the voltage is usually obtained by integrating the electric field in the slot along the shortest path on the substrate surface, impedance definitions vary with the application, and the most appropriate definition must be established on a case-by-case basis. Meinel and Rembold (10) found that the voltage-current definition $Z_{v,i}$ = (Voltage across the slot)/(Current in the fins) was most appropriate for predicting the interaction of finlines with discrete devices, while Knorr and Shayda (14) reported best results with the ridged waveguide definition and Willing and Spielmann (15) preferred the voltage-power definition $Z_{v,p}$ = (Voltage across the slot)/(2 × average power transmitted).

There exist a variety of techniques for the computation of finline parameters, ranging from approximate analytical expressions to sophisticated numerical procedures. They will be outlined briefly in the following. For detailed information the reader is invited to consult to the appropriate references given in the bibliography.

Approximate Methods of Finline Analysis

Since most finlines are made with low-permittivity substrates such as RT-duroid™ ($\epsilon_r = 2.2$) or quartz ($\epsilon_r = 3.75$) that occupies only a small fraction of the waveguide cross-section, their dispersion characteristics can be approximated by the behavior of commensurate waveguides that are filled uniformly with a fictitious frequency-independent dielectric of permittivity $\epsilon_0\epsilon_{re}$ (Fig. 4). (The permittivity of this fictitious dielectric, ϵ_{re}, is called the "equivalent dielectric constant" to distinguish it from the so-called "effective dielectric constant" $\epsilon_{\text{eff}} = (\lambda/\lambda_g)^2$ of a finline.) The uniformly filled ridge waveguide obeys a rather simple dispersion formula for the guided wavelength λ_g and the characteristic impedance Z_0:

$$\lambda_g = \frac{\lambda}{\sqrt{\epsilon_{re} - (\lambda/\lambda_c)^2}}; \quad Z_0 = \frac{Z_\infty}{\sqrt{\epsilon_{re} - (\lambda/\lambda_c)^2}} \tag{2}$$

According to Meier (6) these expressions agree with measurements within ±2% when λ_c and Z_∞ are the cutoff wavelength and characteristic impedance at infinite frequency of an air-filled ridge waveguide of identical dimensions (available from Cohn's (1) or Hopfer's (2) paper, or from other published data), and ϵ_{re} has been determined by measuring the guided wavelength of a test structure at a single frequency in midband (6).

More accurate results can be obtained by the transverse resonance approach that has previously been applied by Cohn (16) and other researchers to analyze ridge waveguides, slab-

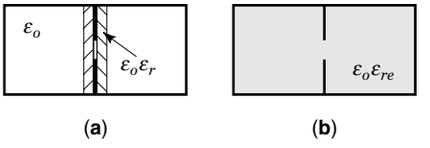

Figure 4. Insulated finline and its equivalent ridged waveguide with identical cross section and uniform dielectric filling of permittivity $\epsilon_0\epsilon_{re}$.

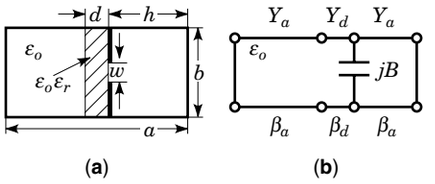

Figure 5. (a) Unilateral finline; (b) and its equivalent transverse network.

loaded waveguides and slotlines. In the simplest formulation, the dominant mode in the finline is considered to be a TE-mode in the transverse direction that resonates between the two sidewalls of the enclosure. In transverse direction, the finline thus appears as a chain of piecewise homogeneous waveguide sections of width $\lambda_g/2$ (λ_g is the wavelength in longitudinal direction of the finline and corresponds to the cutoff wavelength of the transverse waveguide sections). The fins form a capacitive transverse discontinuity. The characteristic admittances and propagation constants of the subsections are those of homogeneous waveguides. The corresponding equivalent circuit is shown in Fig. 5; its transverse resonance condition is obtained by setting the total admittance in the plane of the fins equal to zero

$$\frac{B}{Y_a} - \cot\beta_a h - \frac{Y_d}{Y_a}\cot\beta_d\left\{d + \frac{1}{\beta_d}\tan^{-1}\left[\frac{Y_d}{Y_a}\tan\beta_a(a-d-h)\right]\right\} = 0 \quad (3)$$

where

$$\beta_a = \frac{2\pi}{\lambda}\sqrt{1-(\lambda/\lambda_g)^2},\ \beta_d = \frac{2\pi}{\lambda}\sqrt{\epsilon_r-(\lambda/\lambda_g)^2} \text{ and } \frac{Y_d}{Y_a} = \frac{\beta_d}{\beta_a}$$

By fixing the guided wavelength λ_g and solving Eq. (3) for λ, one obtains the frequencies at which the dominant and higher-order modes propagate down the finline with that wavelength λ_g. The accuracy of the solution depends essentially on the accuracy of the capacitive susceptance B, and the various transverse resonance approaches reported in the literature differ in the way in which this susceptance is determined. They range from quasi-static approximations to variational expressions and mode-matching solutions (17–20). The group of approximate methods also comprises the empirical closed-form equations that are essentially formulas fitted to more accurate numerical results (21,22). Their advantage resides in their simplicity and their suitability for synthesis, but they are limited to certain combinations of parameters and have lost some of their attractiveness due to the proliferation of high-performance computers that yield more rigorous numerical solutions almost instantly.

Rigorous Methods of Finline Analysis

Rigorous methods yield field solutions by solving Maxwell's equations subject to the boundary conditions imposed by the finline geometry. Several are based on the method of moments, from the first formulation in the space domain by Hofmann (23) to the spectral domain approaches described by Itoh (24), Knorr and Shayda (14), and Schmidt and Itoh (25). A mode-matching solution was proposed by Beyer and Wolff (61), and a modified mode-matching approach was presented by Vahldieck and Bornemann (26,27). A singular integral equation formulation was proposed by Omar and Schuenemann (28).

In all these approaches the fields in the dielectric and air-filled subregions of the finline are expressed in terms of rectangular waveguide TE and TM modes resonating in transverse direction, also called Longitudinal Section Electric (LSE) and Longitudinal Section Magnetic (LSM) modes. In fact, each of these modes must satisfy a condition similar to Eq. (3). The modal coefficients are determined such that their superposition satisfies all boundary and interface conditions, in particular, the edge condition at the metal fins where most of the energy in the structure is concentrated. Approaches differ in the way in which the relationship between slot field and fin current distributions is formulated. In the space domain formulation, this relationship takes the form of integral equations. Their kernels are the Green's functions of the housing and substrate without the metal fins. These integral equations are then solved with the method of moments and Galerkin's procedure (identical basis and testing functions are used).

By performing a spatial Fourier transformation of all fields and currents with respect to the coordinates parallel to the substrate plane, one can transform the integral equations into a set of algebraic equations. The resulting spectral domain formulation leads to a very efficient algorithm for the dominant and first higher-order finline eigensolutions and eigenvectors, especially when the slot fields or fin currents are developed into physically realistic basis functions that individually satisfy all the boundary and edge conditions in the plane of the fins. In fact, only a single constant basis function for the slot field is sufficient to determine the dominant wavenumber within 2 to 3%. However, the spectral domain method is restricted to idealized finline geometries (no mounting grooves, zero metallization thickness). It is also less suitable than the singular integral formulation for determining eigensolutions of high order because the set of required basis functions for the slot field or fin current grows quickly in size and complexity.

The general mode matching approach that enforces conservation of tangential field components or complex power across all boundaries between subregions can take these realistic features into account more readily, as can the well-known family of space discrete solution methods, such as the finite difference, finite element and TLM methods of analysis, in both their frequency and time domain formulations, or the method of lines. A detailed description of these methods with extensive bibliographies can be found in Refs. 29 and 30. However, the salient features of the most frequently employed rigorous methods of finline analysis, namely, the spectral domain and the mode-matching methods, will be summarized in the following, together with some typical results.

Spectral Domain Analysis of Finlines. In the spectral domain formulation the Fourier transform of the Green's functions $\tilde{G}_{ij}$ in the finline (expressed in terms of LSE and LSM modes) relates the transforms of the electric field in the slot with those of the current density on the fins via the equation

$$\begin{bmatrix}\tilde{G}_{11}(\alpha_n,\beta,k_0) & \tilde{G}_{12}(\alpha_n,\beta,k_0)\\ \tilde{G}_{21}(\alpha_n,\beta,k_0) & \tilde{G}_{22}(\alpha_n,\beta,k_0)\end{bmatrix}\begin{bmatrix}\tilde{E}_x(\alpha_n)\\ \tilde{E}_z(\alpha_n)\end{bmatrix} = \begin{bmatrix}\tilde{J}_x(\alpha_n)\\ \tilde{J}_z(\alpha_n)\end{bmatrix}$$

$$\tilde{G}_{11} = -(\alpha_n^2 Z_{\text{LSE}} + \beta_n^2 Z_{\text{LSM}})/(\alpha_n^2+\beta_n^2) \quad (4)$$

$$\tilde{G}_{12} = \tilde{G}_{21} = -\alpha_n\beta_n(Z_{\text{LSE}} - Z_{\text{LSM}})/(\alpha_n^2+\beta_n^2)$$

$$\tilde{G}_{22} = -(\alpha_n^2 Z_{\text{LSE}} + \beta_n^2 Z_{\text{LSM}})/(\alpha_n^2+\beta_n^2)$$

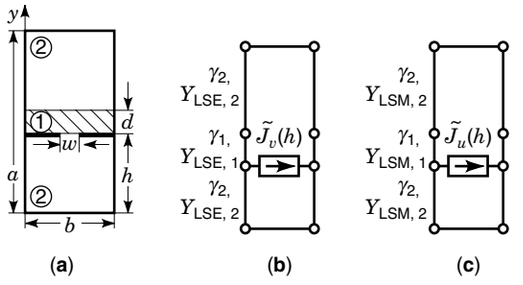

Figure 6. Cross section of a unilateral finline (a) and its equivalent transverse modal circuits for LSE (b) and LSM (c) modes.

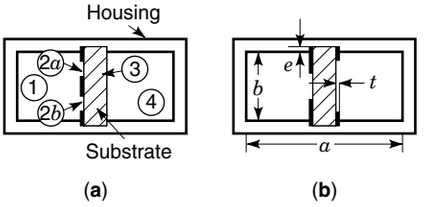

Figure 8. Two basic finline structures with finite metallization and substrate mounting grooves; t = finite metallization thickness, e = depth of mounting grooves, a = waveguide width, b = waveguide height. (a) Edge-coupled unilateral finline, (b) Asymmetric bilateral finline.

where Z_{LSE} and Z_{LSM} are the impedances seen from the nodes of the current source, looking into the respective equivalent circuits of Fig. 6(b) and (c). α_n is the Fourier variable, $\beta = 2\pi/\lambda_g$ is the propagation constant in the axial direction, and k_0 is the free-space wavenumber; $\tilde{E}_x$, $\tilde{E}_z$, $\tilde{J}_x$ and $\tilde{J}_z$ are the electric fields in the slot and the current densities on the fins, respectively. This relationship is most readily formulated using Itoh's (24) immittance approach. Figure 6 shows the cross section of a unilateral finline, together with the equivalent transverse modal circuits for the immittance formulation of the Green's functions. The slot fields and fin currents are expressed in terms of known basis functions with unknown coefficients. Applying Galerkin's procedure and Parceval's theorem results in a set of algebraic equations. The roots of the characteristic equation yield the eigenvalues of the finline.

The method is particularly efficient when basis functions are selected that satisfy already the edge condition at the fins. Thus, only a few basis functions are necessary to accurately describe the field in the slot or the current density on the fins. Once the coefficients of the basis functions are determined, the field functions inside the structure can be derived, and quantities such as slot voltage, fin current and characteristic impedances can be determined by appropriate integration over the field functions. Figure 7 shows the effective dielectric constant and voltage-power impedance of the unilateral finline in Fig. 6, computed with a single constant basis function for E_x in the slot. The enclosure is a standard WR-28 rectangular waveguide.

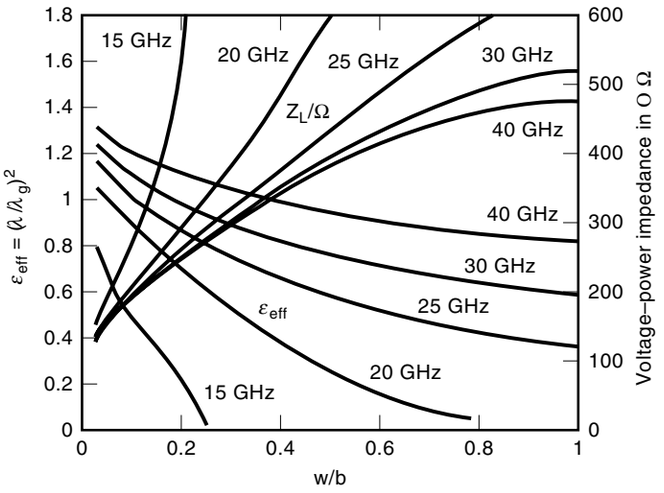

Figure 7. Effective dielectric constant and voltage-power impedance of the unilateral finline shown in Fig. 6, computed with the spectral domain method using a single constant basis function for the slot field E_x. The dimensions are: a = 7.112 mm; b = 3.556 mm; h = 3.429 mm; d = 0.254 mm; ϵ_r = 2.2.

As mentioned earlier, geometrical details such as the substrate mounting grooves and finite metallization thickness must be accounted for in practical realizations, particularly at higher frequencies. These can easily be included in the mode-matching analysis. Representative finline characteristics obtained with this approach will be presented in the following as well.

Two typical finline structures with realistic geometrical details are presented in Fig. 8. Depending on the application, structures that support quasi-TEM modes [Fig. 8(a)] or configurations with pure slotline layout [Fig. 8(b)] are utilized. The principal difference between the two types is that in the first the dominant mode of propagation is the quasi-TEM mode without a lower cutoff frequency, while in the slotline structure the dominant mode is limited by a cutoff frequency that is determined mainly by the width of the slot(s).

Both types of finlines carry hybrid modes due to the presence of the dielectric substrate that supports the fins. Hybrid modes are neither TE nor TM but a combination of both, denoted as either HE or EH modes with all six field components present; HE modes are those with a predominant H_z field component, while EH modes exhibit a stronger E_z field component. Only at cutoff are these modes purely of type TE or TM. These modes often carry the same indices as TE and TM modes, such as HE_{nm} or EH_{nm}, indicating that the latter two originate from the corresponding TE or TM modes at cutoff. At frequencies above cutoff, the field configuration of the individual hybrid modes can differ significantly from the TE and TM modes. Therefore, hybrid modes are equally often numbered according to the sequence at which they occur, such as HE_n and EH_m.

In the mode-matching approach, the finite metallization thickness and substrate mounting grooves are taken into account from the outset. It yields a somewhat longer guided wavelength than spectral domain analysis since a higher percentage of the electric field travels in air within the slot region. The hybrid modes are derived from the z-components of the magnetic and electric vector potentials $\vec{\phi}_h$ and $\vec{\theta}_e$, respectively

$$\vec{E} = \nabla \times \vec{\varphi}_{hz} + \frac{1}{j\omega\epsilon}\nabla \times \nabla \times \vec{\theta}_{ez}$$
$$\vec{H} = \nabla \times \vec{\theta}_{ez} - \frac{1}{j\omega\epsilon}\nabla \times \nabla \times \vec{\varphi}_{hz} \tag{5}$$

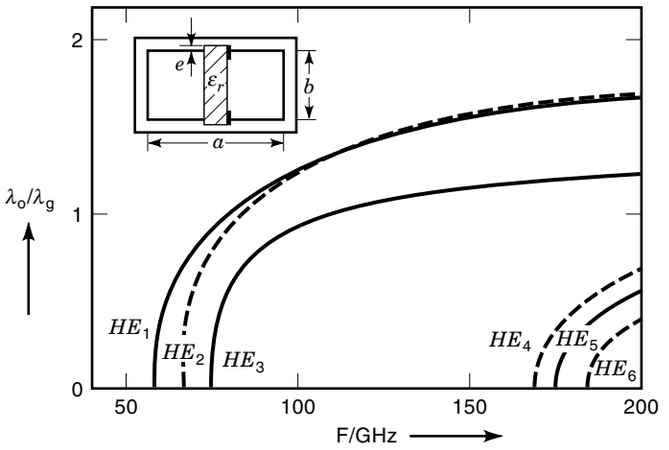

Figure 9. Dispersion characteristics of the first six hybrid eigenmodes in a unilateral finline. The dashed curves indicate modes that are not excited by the incident TE_{10} mode. The dimensions are: a = 1.65 mm; $b = a/2$, e = 0.5 mm; t = 5 μm, ϵ_r = 3.75. (After Vahldieck (23), Copyright © 1984 IEEE, reprinted with permission.)

where

$$\varphi_{hz} = \sum_n Q_n^h(x) f_n(y) e^{-j\beta_n z}$$
$$\theta_{ez} = \sum_n P_n^e(x) g_n(y) e^{-j\beta_n z} \tag{6}$$

Q, P, f and g denote transverse eigenfunctions defined in each subregion of the finline cross-section [i.e., regions 1, 2a, 2b, 3, 4 in Fig. 8(a)]. The electric and magnetic field tangential to the interfaces between the subregions is proportional to the vector potentials and its derivatives

$$E_y \propto \frac{dQ^h}{dx} = P^h, E_z \propto P^e, H_z \propto Q^h, H_y \propto \frac{dP^e}{dx} = Q^e \tag{7}$$

Matching the tangential field components at each interface and utilizing the orthogonality of modes leads to one coupling matrix ($C\mu$ for μ = 1, 2a, 2b, 3, 4) per interface. The coupling matrices can be linked successively by transferring the electric and magnetic fields from one boundary of a subregion to the opposite one. These transfer matrices ($T\mu$ for μ = 1, 2a, 2b, 3, 4) are the generalized (fundamental and higher-order modes) transmission line equations in each subregion. The resulting matrix equation yields

$$\begin{bmatrix} P^h = 0 \\ P^e = 0 \\ Q^h \\ Q^e \end{bmatrix}_{x=0} = \underbrace{\prod_{n=1}^{n=3} T^n C^n T^4}_{G} \begin{bmatrix} P^h = 0 \\ P^e = 0 \\ Q^h \\ Q^e \end{bmatrix}_{x=a} \tag{8}$$

From the resonance condition in Eq. (8) the characteristic equation G_{12} is obtained. Solving for $det(G_{12}) = 0$ yields the propagation constant β or guided wavelength λ_g. Typical dispersion characteristics obtained in this way for the first six eigenmodes in a unilateral finline are shown in Fig. 9. The modes that are not excited by an incident TE_{10} mode are dashed. The first important higher-order mode is thus HE_3; the single-mode bandwidth of the dominant mode is situated between the cutoff frequencies of HE_1 and HE_3 (frequencies at which the curves intersect the frequency axis). Note that these dispersion curves change with both the groove depth e and the metallization thickness t as shown in the following.

Effect of Mounting Grooves. Mounting grooves are required to hold the substrate in the waveguide housing. A detailed analysis of the effect of the groove depth on the modes is given in Refs. 26 and 31. It was found that for unilateral finlines the cutoff frequencies of higher-order modes react very sensitively to the groove depth (e in Fig. 8), which for one-fifth of the waveguide height reduces the cutoff frequency of higher-order modes to such an extent that the finline is useless for most practical purposes. This is due to modes that originate from the TE_{20} (HE_3) and TE_{01} (HE_2) modes of the empty waveguide. Both modes appear to be coupled, are highly concentrated between the metallization within the substrate, and are thus very sensitive to changes in the groove depth. This effect is particularly pronounced in Fig. 10. The asymmetric bilateral finline carries an additional metallic strip inside the gap on the right-hand side of the substrate. For centered finlines this interaction between modes is greatly reduced since some of them will not be excited. This is not the case for unilateral finlines. However, since the metallization is only on one side of the substrate, the problem is not as pronounced.

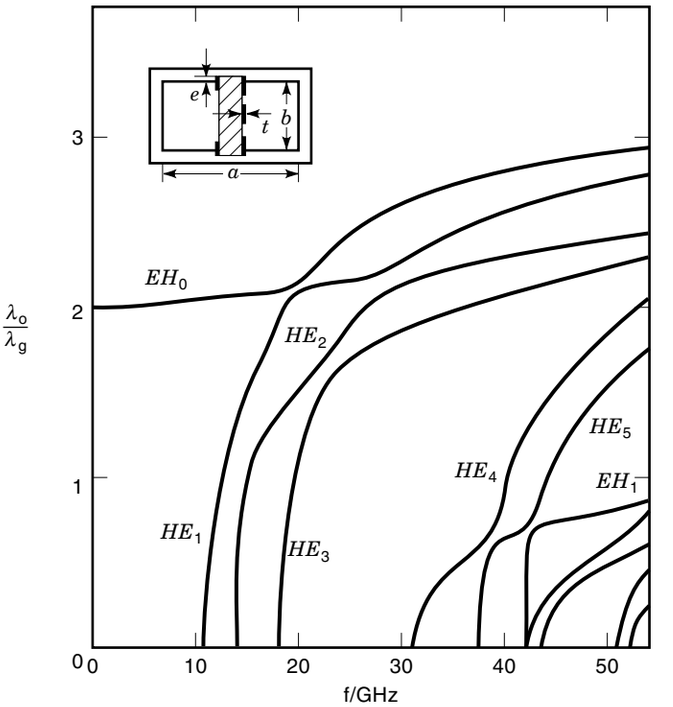

Figure 10. Dispersion characteristics of an asymmetric bilateral finline with an additional metallic strip in the gap on the right-hand side of the substrate. The modes appear to be strongly coupled and are very sensitive to changes in the groove depth. The dimensions are: a = 7.112 mm; b = 3.556 mm; e = 0.7 mm; t = 71 μm, ϵ_r = 10. (After Vahldieck and Bornemann (24), Copyright © 1985 IEEE, reprinted with permission.)

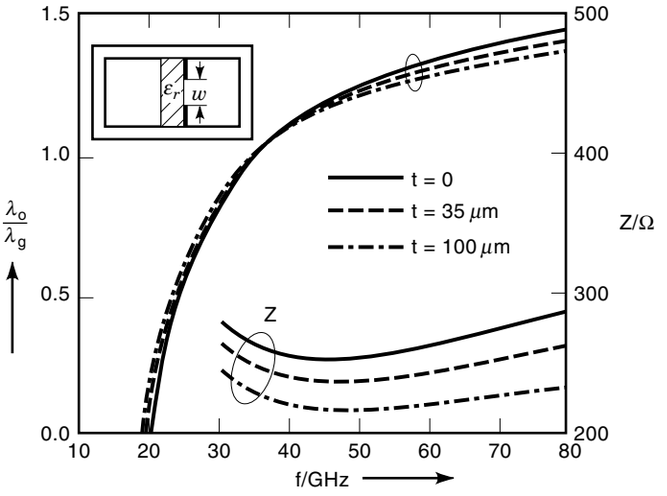

Figure 11. Effect of metallization thickness on the dispersion characteristics and the characteristic impedance of a unilateral finline. The dimensions are: $a = 4.776$ mm; $b = 2.388$ mm; $d = 0.127$ mm; $w = 0.2b$; $\epsilon_r = 3.8$. (After Kitazawa and Mittra (54), Copyright © 1984 IEEE, reprinted with permission.)

Effect of Finite Metallization Thickness. The effect of finite metallization on the propagation constant and the characteristic impedance has been investigated by several researchers (26,31–33,62). A typical behavior of the dominant mode in a unilateral finline with three different values of metallization thickness is shown in Fig. 11. The effect of mounting grooves is not included here. The characteristic impedance is reduced throughout the operating bandwidth when the metallization becomes thicker. This is consistent with the behavior of the ridge waveguide (1,2) where the capacitive loading of the waveguide increases when the ridge becomes wider. However, the propagation constant is not affected in the same way at lower and at higher frequencies. While the cutoff frequency is reduced by thicker metallization for the same reason as the characteristic impedance, the effect is reversed at higher frequencies; because of the wider air gap between thicker fins, more of the field energy travels in the air gap and less is concentrated in the dielectric, leading to a higher phase velocity. As a result, there is a crossover of the dispersion curves at midband. In conclusion, the effect of finite metallization on the propagation constant is minimal around the center of the operating bandwidth.

FINLINE DISCONTINUITIES

Discontinuities in the finline geometry form the building blocks of finline circuits. Given the many degrees of freedom in the design of finlines, the possibilities are endless, and it would be impossible to give a complete treatment of this subject. Nevertheless, one can identify some generic types of finline discontinuities and provide some basic characteristics. Some of the most important are: inductive strips; step changes in gap width; notches; dents; and series stubs. The shapes of typical discontinuities are shown in Fig. 12, together with their equivalent lumped element networks. Note that, in contrast to similar waveguide discontinuities, the circuit elements are determined solely by the metallization pattern of the planar insert, while the geometry of the enclosure remains unchanged. This results in a considerable reduction in the manufacturing cost, as the discontinuities are realized using printed circuit techniques rather than machining.

The effect of discontinuities on the guided wave in the finline can be represented either by generalized scattering parameters (S-parameters) or by equivalent lumped networks. These are not determined solely by the local changes of the dominant waveguiding parameters, but include the effects of mode conversion, energy storage and possibly multimode interactions between neighboring discontinuities. Within the single-mode propagation range, dominant mode S-parameters are sufficient to describe the behavior of discontinuities, provided that they have been determined at reference planes beyond the reach of evanescent higher-order modes.

The theoretical characterization of finline discontinuities is a challenge for the same reasons as the computation of finline

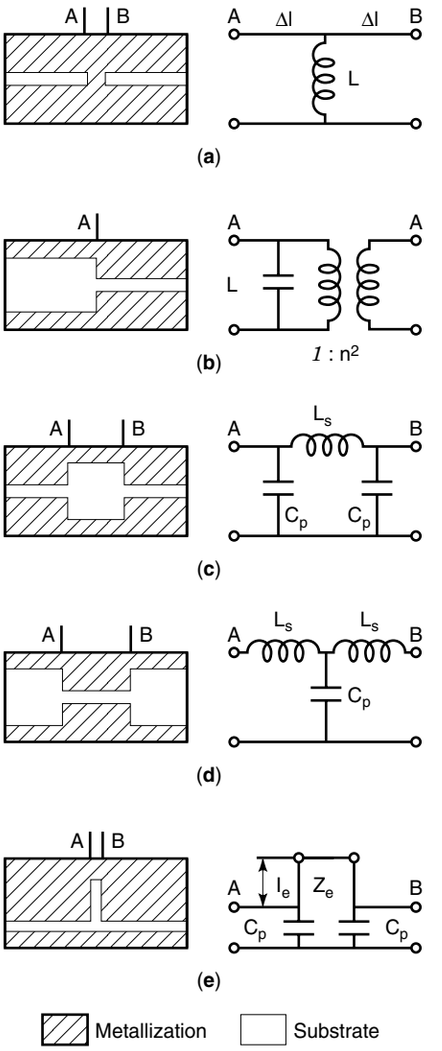

Figure 12. Profile of some important finline discontinuities and their equivalent lumped element circuits. (a) Inductive strip, (b) Impedance step (step change in gap width), (c) Inductive notch, (d) Capacitive strip, (e) Series stub. Note that the distance between planes A and B is short compared to the wavelength.

characteristics. Inhomogeneous dielectric filling and edge singularities call for special approaches, ranging from experimental (6,34–36) over variational (37) and spectral domain techniques (35,38,39) to mode-matching in longitudinal (40–42) as well as in transversal (43) directions.

Inductive Strips

Inductive strips are important elements of bandpass filters. Meier (6) has determined the equivalent shunt inductance of strips from insertion loss measurements and from the resonant frequency of a one-section filter. Pic and Hoefer (34) have characterized strips and impedance steps by measuring the shift they caused in the resonant frequencies of an oversized cavity. The resulting empirical formulas for the strip inductance were confirmed by spectral domain evaluations performed by Koster and Jansen (39). Further methodologies for the characterization of inductive strips and related discontinuities can be found in papers by Knorr and Deal (35), Zhang and Itoh (38), Saad and Schuenemann (44) and Omar and Schuenemann (45). To achieve maximum Q-factors in bandpass filters formed by inductive strips, the gap width of the resonant sections is usually maximized to the full height b of the enclosure. Such full-height strips and their interactions have been analyzed extensively with mode-matching techniques by Arndt et al. (46) and Shih et al. (47), leading to highly accurate CAD programs for E-plane bandpass filters.

Single and Interacting Impedance Steps

These discontinuities are formed by sudden changes in the gap width and come in many shapes and forms [Fig. 12(b)–(d)]. They serve as impedance transformers, tuning and matching elements, mounting platforms for semiconductor devices, or constitutive elements of filters. Besides empirical characterization (34), most systematic analytical approaches employ the representation of fields near the discontinuities by eigenmodes of either the adjacent uniform finline subsections (mode-matching in longitudinal direction) or of transverse homogeneous waveguide subsections. As mentioned earlier, the former approach requires the determination of the eigensolutions of the finline subsections. It has been pointed out by Omar and Schuenemann (45) that the spectrum of finline modes can contain pairs of complex eigensolutions, and that their omission in the modal decomposition of the fields at the discontinuity can lead to significant errors. Various analyses and properties of impedance steps have also been described by El Hennawy and Schuenemann (40,41), Helard et al. (42), Sorrentino and Itoh (43) and Beyer (48).

Narrow Series Slots

The series slot [Fig. 12(e)] is a popular tuning element in the design of oscillators and lowpass filters. It can be represented by a series-connected transmission line of effective length l_e and two stray capacitances that account for the field energy stored in the stray field at the junction. The effective length includes the stray effect at the end of the slot. Burton and Hoefer (49) have characterized such slots experimentally and have given closed-form expressions for the elements of the equivalent circuit in Fig. 2(e). These expressions are valid over an entire waveguide band and are independent of the dimensions of the enclosure. This indicates that narrow slots in the finline metallization behave essentially like slotline elements (16).

TRANSITIONS TO OTHER TRANSMISSION MEDIA

Most practical finline circuits include one or several types of transitions, either between different types of finlines or between finlines and other transmission media such as rectangular waveguides, coaxial line or microstrip. Of particular importance and interest is the transition between finline and the commensurate rectangular waveguide due to the need to interface finline circuits with measurement systems and conventional components. Transitions between different finline types and also between finlines and other planar circuits are needed to combine them and to take advantage of their respective properties in an integrated design. The topologies and properties of such transitions will be summarized in the following.

Transitions Between Finline and Waveguide

Transitions between finline and the commensurate rectangular waveguide are realized by varying in some way the slot between the full height of the waveguide and the final slot width. The bandwidth and the VSWR of the transition depend entirely on the profile of the fin contour and the length of the transition. The geometrically simplest transition is a linear taper extending over at least three guided wavelengths, as used by Cohen and Meier (13). More sophisticated designs that are shorter than a wavelength employ single or double exponential profiles, cosine profiles, parabolic and circular profiles, as well as other profiles derived by nonuniform transmission line theory (50–53). Figure 13 shows some typical taper profiles employed for the realization of finline-to-waveguide transitions.

The problem of taper optimization amounts to realizing the lowest possible insertion loss over a given frequency band with a taper of minimum length. A rigorous treatment of the tapered transition leads to a nonlinear differential equation of the Riccati type that must be solved numerically. Approximate solutions can be found, however, yielding the so-called Dolph-Chebyshev taper (51). This taper has impedance discontinuities at its extremities that introduce parasitic reactances. However, since it is impossible to uniquely define the local characteristic impedance of a tapered finline, one might as well select a profile that approximates the "optimal" contour. Indeed, most researchers who have measured the characteristics of such tapers agree that the profile is not very critical, especially when the taper is about a wavelength long or more.

Detailed formulas and instructions for the synthesis of finline tapers have been reported by Hinken (50), Schieblich et al. (51), Beyer and Wolff (52), and Pramanick and Bhartia (53). A transition comprising a short finline taper with a circular contour and matching capacitive discontinuities has been proposed by de Ronde (54), who claims that its performance is similar to that of an optimized taper, but its length does not exceed 3/8ths of λ_{max}. Typical finline tapers have a return loss better than 20 dB over a standard waveguide band.

One feature that cannot be neglected in most applications is the discontinuity introduced by the finline substrate itself.

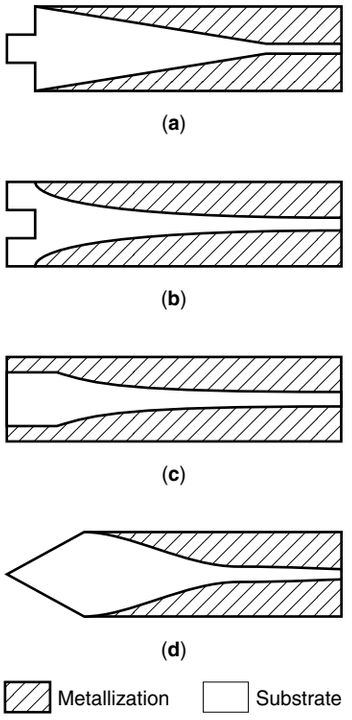

Figure 13. Profile of typical finline tapers and matching elements for the reduction of reflections from the dielectric slab interface. (a) Linear taper with quarterwave substrate protrusion, (b) Exponential taper with quarterwave substrate notch, (c) Exponential taper with printed quarterwave section, (d) Double circular profile taper with triangular substrate protrusion.

When the slotwidth is equal to the waveguide height, the finline becomes a dielectric slab-loaded waveguide. The reflection due to the substrate alone deteriorates the return loss of a subsequent taper typically by 5 dB. Cohen and Meier (13) reduced these spurious reflections by cutting a quarterwave notch into the dielectric substrate with dimensions determined experimentally. Verver and Hoefer (55) later developed closed-formed expression for the design of such notches and their dual, dielectric protrusions. Drawings by Piotrowski and Wojtasiak (56) and by Beyer et al. (36) show transitions with triangular protrusions of the substrate, but no design information is given. For hard substrates that are difficult to cut (quartz), a printed transformer structure consisting of one or even two quarterwave sections in front of the taper is more appropriate (57). Figure 13 shows how such matching elements can be incorporated in the design of a finline taper.

Transitions Between Finlines and Other Planar Media

Many transitions between various types of finlines (58) as well as between finlines and other planar media such as microstrip, coplanar waveguide, and suspended and inverted microstrip have been developed. A good survey of such transitions can be found in by Bhat and Koul (11). The topologies are rather difficult to analyze and thus have been optimized empirically. Care must be taken not to excite unwanted modes and to avoid resonances that can considerably affect the transfer function of such transitions (59).

CONCLUSION

The principal advantages of finline technology at millimetric frequencies are wide single-mode bandwidth, moderate insertion loss, freedom from radiation and interference, suitability for batch processing and low-cost production in both small and large quantities, potential for circuit integration, and compatibility with waveguide instrumentation. When properly constructed, finline components are rugged and reliable, withstanding considerable thermal and mechanical stress. Practically all imaginable circuit functions have been realized thanks to the many advances in the field-theoretical modeling of quasi-planar circuits. While early design efforts relied mostly on approximate and empirical characterization of finlines, rigorous formulations of the field problem and their numerical implementations have made it possible to design, optimize and fabricate finline components entirely by computer.

The major drawback of the finline is its limited compatibility with transistors. On the other hand, active and passive diodes are easily embedded into a finline; oscillators, frequency converters, switches, phase shifters and attenuators with excellent performance have thus been realized. Entire integrated millimeter-wave radar front ends for frequencies up to 140 GHz have been built by the finline technique, demonstrating the potential and versatility of this technology that favorably combines the high electrical quality of the waveguide with the advantages of planar circuitry. When paired with the available computer-based design tools, finline stands out as an important and versatile technology in the arsenal of the modern microwave and millimeter-wave engineer.

FURTHER READING

The literature on finlines is quite extensive; only a small number of key references could be cited here. The reader in search for more detailed information is referred to the comprehensive survey papers by Solbach (9) and by Meier (60). Bhartia and Pramanick (12) have assembled a collection of reprints of key papers on E-plane integrated circuits. Finally, in their book on the analysis, design and applications of finlines, Bhat and Koul (11) have gathered and organized a wealth of design information, methods and references on the subject. Further details on numerical techniques for the analysis of microwave circuits and electromagnetic wave problems can be found in two volumes edited by Itoh (29) and Yamashita (30).

BIBLIOGRAPHY

1. S. B. Cohn, Properties of ridge waveguide, *Proc. IRE,* **35**: 783–788, 1947.
2. S. Hopfer, The design of ridge waveguides, *IRE Trans. Microw. Theory Tech.,* **MTT-3**: 20–29, 1955.
3. S. D. Robertson, The ultra-bandwidth finline coupler, *Proc. IRE,* **43**: 739–788, 1955.
4. Y. Konishi and N. Hoshino, 100-GHz-band low-noise mixer, *Inst. Electr. Commun. Eng., Jpn.,* **MMW 71**: July 1971.
5. P. J. Meier, Two new integrated-circuit media with special advantages at millimeter wavelengths, *1972 IEEE MTT Int. Microw. Symp. Dig.,* Arlington Heights, IL, 1972, pp. 221–223.

6. P. J. Meier, Integrated finline millimeter components, *IEEE Trans. Microw. Theory Tech.,* **MTT-22**: 1209–1216, 1974.
7. P. J. Meier, *Microwave transmission line,* U.S. Patent 3 825 863, 1974.
8. B. Adelseck et al., A survey of planar integrated mm-wave components, *Radio Electron. Eng.,* **45**: 46–50, 1982.
9. K. Solbach, The status of printed millimeter-wave E-plane circuits, *IEEE Trans. Microw. Theory Tech.,* **MTT-31**: 107–121, 1983.
10. H. Meinel and B. Rembold, New millimeter-wave fin-line attenuators and switches, *1979 IEEE MTT-S Int. Microw. Symp. Dig.,* Orlando, FL, 1979, pp. 249–252.
11. B. Bhat and S. K. Koul, *Analysis, Design and Applications of Fin Lines,* Norwood, MA: Artech House, 1987.
12. P. Pramanick and P. Bhartia, *E-Plane Integrated Circuits,* Norwood, MA: Artech House, 1987.
13. L. D. Cohen and P. J. Meier, Advances in E-plane printed millimeter-wave circuits, *IEEE MTT-S Int. Microw. Symp. Dig.,* 1978, pp. 27–29.
14. J. Knorr and P. Shayda, Millimeter-wave fin-line characteristics, *IEEE Trans. Microw. Theory Tech.,* **MTT-28**: 737–743, 1983.
15. H. A. Willing and B. E. Spielman, Experimental assessment of bilateral fin-line impedance for device matching, *1981 IEEE MTT-S Int. Microw. Symp. Dig.,* Los Angeles, CA, 1981, pp. 105–107.
16. S. B. Cohn, Slot-line on a dielectric substrate, *IEEE Trans. Microw. Theory Tech.,* **MTT-17**: 768–778, 1969.
17. A. M. K. Saad and G. Begemann, Electrical performance of finlines of various configurations, *IEE Proc. Microw., Opt., Acoust.,* Part H, **1**: 81–88, 1977.
18. W. J. R. Hoefer, Finline design made easy, *1978 IEEE MTT Int. Microw. Symp. Dig.,* Ottawa, ON, 1978, p. 471.
19. R. N. Simons, Analysis of millimetre-wave integrated fin line, *IEE Proc. Microw., Opt., Acoust.,* part H, **130**: 1983, pp. 166–169.
20. J. K. Piotrowski, Accurate and simple formulas for dispersion in finlines, *1984 IEEE MTT Int. Microw. Symp. Dig.,* San Francisco, CA, 1984, pp. 333–336.
21. A. K. Sharma and W. J. R. Hoefer, Empirical expressions for finline design, *IEEE Trans. Microw. Theory Tech.,* **MTT-31**: 350–356, 1983.
22. P. Pramanick and P. Bhartia, Computer-aided design models for millimeter-wave finlines and suspended substrate microstrip lines, *IEEE Trans. Microw. Theory Tech.,* **MTT-35**: 1429–1435, 1985.
23. H. Hofmann, Dispersion of planar waveguides for millimeter-wave applications, *Arch. Elek. Übertragung,* **31**: 40–44, 1977.
24. T. Itoh, Spectral domain immittance approach for dispersion characteristics of generalized printed transmission lines, *IEEE Trans. Microw. Theory Tech.,* **MTT-28**: 733–736, 1980.
25. L.-P. Schmidt and T. Itoh, Spectral domain analysis of dominant and higher order modes in fin-lines, *IEEE Trans. Microw. Theory Tech.,* **MTT-28**: 981–985, 1980.
26. R. Vahldieck, Accurate hybrid mode analysis of various finline configurations including multilayered dielectrics, finite metallization thickness and substrate holding grooves, *IEEE Trans. Microwave Theory Tech.,* **MTT-32**: 1454–1460, 1984.
27. R. Vahldieck and J. Bornemann, A modified mode-matching technique and its application to a class of quasi-planar transmission lines, *IEEE Trans. Microw.Theory Tech.,* **MTT-33**: 916–926, 1985.
28. A. Omar and K. Schuenemann, Formulation of the singular integral equation technique for planar transmission lines, *IEEE Trans. Microw. Theory Tech.,* **MTT-33**: 1313–1321, 1985.
29. T. Itoh, *Numerical Techniques for Microwave and Millimeter-Wave Passive Structures,* New York: Wiley, 1989.
30. E. Yamashita, *Analysis Methods for Electromagnetic Wave Problems,* Norwood, MA: Artech House, 1990.
31. R. Vahldieck and W. J. R. Hoefer, The influence of metallization thickness and mounting grooves on the characteristics of fin lines, *IEEE MTT Int. Microw. Symp. Dig.,* St. Louis, MO, 1985, pp. 143–144.
32. T. Kitazawa and R. Mittra, Analysis of finline with finite metallization thickness, *IEEE Trans. Microw. Theory Tech.,* **MTT-32**: 1484–1487, 1984.
33. J. K. Piotrowski, Efficient analysis of finline with finite metallization thickness, *IEEE MTT-S Int. Microw. Symp. Dig.,* 1986, pp. 213–216.
34. E. Pic and W. J. R. Hoefer, Experimental characterization of fin line discontinuities using resonant techniques, *IEEE MTT Int. Microw. Symp. Dig.,* Los Angeles, CA, 1981.
35. J. B. Knorr and J. C. Deal, Scattering coefficients of an inductive strip in a fin-line: theory and experiment, *IEEE Trans. Microw. Theory Tech.,* **MTT-33**: 1011–1017, 1985.
36. A. Beyer, D. Köther, and I. Wolff, A combined theoretical and experimental characterization of discontinuities in unilateral finlines, *IEEE MTT Int. Microw. Symp. Dig.,* Baltimore, 1986, pp. 127–130.
37. K. J. Webb and R. Mittra, A variational solution of the finline discontinuity problem, *15th Eur. Microw. Conf. Dig.,* 1985, pp. 311–316.
38. Q. Zhang and T. Itoh, Spectral domain analysis of scattering from E-plane circuit elements, *IEEE Trans. Microw. Theory Tech.,* **MTT-35**: 138–150, 1987.
39. N. H. L. Koster and R. H. Jansen, Some new results on the equivalent circuit parameters of the inductive strip discontinuity in unilateral fin-lines, *Arch. Elek. Übertragung,* **35**: 497–499, 1981.
40. H. El Hennawy and K. Schuenemann, Analysis of fin-line discontinuities, *IEE Proc.,* **129**: 342–350, 1982.
41. H. El Hennawy and K. Schuenemann, Impedance transformation in fin lines, *9th Eur. Microw. Conf. Dig.,* 1979, pp. 448–452.
42. M. Helard et al., Solution of fin-line discontinuities through the identification of its first four higher order modes, *IEEE MTT Int. Microw. Symp. Dig.,* 1983, pp. 387–389.
43. R. Sorrentino and T. Itoh, Transverse resonance analysis of finline discontinuities, *IEEE MTT-S Int. Microw. Symp. Dig.,* 1984, pp. 414–415.
44. A. M. K. Saad and K. Schuenemann, A rectangular waveguide equivalent for bilateral and unilateral finlines, *Arch. Elek. Übertragung,* **35**: 287–292, 1981.
45. A. S. Omar and K. Schuenemann, Transmission-matrix representation of fin-line discontinuities, *IEEE MTT-S Int. Microw. Symp. Dig.,* 1984, pp. 339–341.
46. F. Arndt et al., Theory and design of low-insertion loss fin-line filters, *IEEE Trans. Microw. Theory Tech.,* **MTT-30**: 155–163, 1982.
47. Y. C. Shih, T. Itoh, and L. Q. Bui, Computer-aided design of millimeter-wave e-plane filters, *IEEE Trans. Microw. Theory Tech.,* **MTT-31**: 135–142, 1983.
48. A. Beyer, Calculation of discontinuities in grounded fin lines taking into account the metallization thickness and the influence of the mount-slits, *12th Eur. Microw. Conf. Dig.,* 1982, pp. 681–686.
49. M. Burton and W. J. R. Hoefer, An improved model for short- and open-circuited series stubs in fin lines, *IEEE MTT-S Int. Microw. Symp. Dig.,* 1984, pp. 330–332.
50. J. H. Hinken, Simplified analysis and synthesis of finline tapers, *Arch. Elek. Übertragung,* **37**: 375–380, 1983.
51. C. Schieblich, J. K. Piotrowski, and J. H. Hinken, Synthesis of optimum finline tapers using dispersion formulas for arbitrary slot widths and locations, *IEEE Trans. Microw. Theory Tech.,* **MTT-32**: 1638–1645, 1984.

52. A. Beyer and I. Wolff, Finline taper design made easy, *IEEE MTT-S Int. Microw. Symp. Dig.,* 1985, pp. 493–496.
53. P. Pramanick and P. Bhartia, Analysis and synthesis of tapered finlines, *Microw. RF,* **26**: 111–114, 1987.
54. F. C. de Ronde, Miniaturization in E-plane technology, *15th Eur. Microw. Conf. Dig.,* 1985, pp. 329–333.
55. C. J. Verver and W. J. R. Hoefer, Quarter wave transformers for matching transitions between waveguides and fin lines, *IEEE MTT-S Int. Microw. Symp. Dig.,* 1984, pp. 417–421.
56. J. K. Piotrowski and W. Wojtasiak, A waveguide-to-microstrip transition, *16th Eur. Microw. Conf. Dig.,* 1986, pp. 505–510.
57. W. J. R. Hoefer and C. J. Verver, Optimal waveguide to E-plane circuit transitions with binomial and Chebyshev transformers, *15th Eur. Microw. Conf. Dig.,* 1985, pp. 305–310.
58. H. El Hennawy and K. Schuenemann, Hybrid finline matching structures, *IEEE Trans. Microw.Theory Tech.,* **MTT-30**: 2132–2138, 1982.
59. K. Solbach, H. Callsen, and W. Menzel, Spurious resonances in asymmetrical finline junctions, *IEEE Trans. Microw. Theory Tech.,* **MTT-29**: 1193–1195, 1981.
60. P. J. Meier, Integrated finline, the second decade, *Microw. J.,* **28** (12): 30–48, 1985.
61. A. Beyer and I. Wolff, A solution of the earthed fin line with finite metallization thickness, *1980 IEEE MTT-S Int. Microw. Symp. Dig.,* Washington DC, pp. 258–260.
62. A. Beyer, Analysis of the characteristics of an earthed fin line, *IEEE Trans. Microw. Theory Tech.,* **MTT-29**: 676–680, 1981.

WOLFGANG J. R. HOEFER
University of Victoria

RUEDIGER VAHLDIECK
Institut für Feldtheorie und
Höchstfrequenztechnik